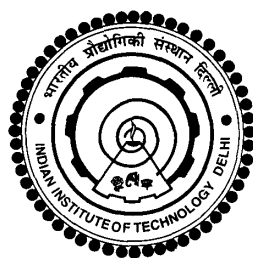


COMPUTER SIMULATIONS OF FREE
ENERGY LANDSCAPES OF PEPTIDES,
THEIR HYDRATION BEHAVIOR AND
METAL SURFACE DEACTIVATION

MADHULIKA GUPTA



DEPARTMENT OF CHEMISTRY
INDIAN INSTITUTE OF TECHNOLOGY DELHI
JANUARY 2018

COMPUTER SIMULATIONS OF FREE
ENERGY LANDSCAPES OF PEPTIDES,
THEIR HYDRATION BEHAVIOR AND
METAL SURFACE DEACTIVATION

by

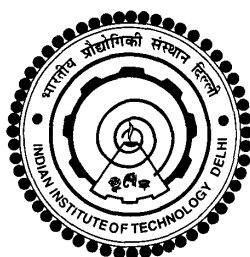
MADHULIKA GUPTA

DEPARTMENT OF CHEMISTRY

Submitted

in fulfillment of the requirements of the degree of Doctor of Philosophy

to the



INDIAN INSTITUTE OF TECHNOLOGY DELHI

JANUARY 2018

Dedicated To My Parents,
Nani, (Late) Nanaji and
(Late) Prof. Charusita Chakravarty

Certificate

This is to certify that the thesis titled "**COMPUTER SIMULATIONS OF FREE ENERGY LANDSCAPES OF PEPTIDES, THEIR HYDRATION BEHAVIOR AND METAL SURFACE DEACTIVATION**" is being submitted by **Ms. Madhulika Gupta** to the Department of Chemistry, Indian Institute of Technology Delhi, for the award of the degree of **Doctor of Philosophy**. This thesis is a record of bona-fide research work carried out by her under the supervision of (Late) Prof. Charusita Chakravarty from 2 January, 2012 to 29 March, 2016 and subsequently under our guidance. In our opinion, the thesis has reached the standards fulfilling the requirements of the regulations relating to the degree.

The results contained in this thesis have not been submitted to any other university or institute for the award of any degree or diploma.

Prof. Pramit Chowdhury
Associate Professor
Department of Chemistry
Indian Institute of Technology Delhi
New Delhi-110016, India

Prof. Sanjoy Bandyopadhyay
Professor
Department of Chemistry
Indian Institute of Technology Kharagpur
Kharagpur-721302, India

Prof. M. Ali Haider
Assistant Professor
Department of Chemical Engineering
Indian Institute of Technology Delhi
New Delhi-110016, India

ACKNOWLEDGEMENTS

I would like to thank God for bestowing me with his blessings and for instilling me with the courage and strength for tomorrow's challenges. I also thank all the people who have unknowingly contributed to this thesis.

First and foremost, I whole-heartedly thank my supervisor and mentor, (Late) Prof. Charusita Chakravarty who has been a role model and nurtured my research career since my graduation days. I feel overwhelmed and honored to work under her guidance during my summer projects as well as my Ph.D. life. She groomed my career with her words of encouragement, personal experiences, perseverance and moral support. She is an integral part of my life and I will always count myself lucky to be her student and to share countless memorable moments with her. She transformed my weaknesses to strengths, from grass to grace and from nothing to something. She was an icon of integrity and hard work and I look forward for carrying her legacy in future.

I am indebted to Prof. Ramakrishna Ramaswamy for his unflinching support and for leading my path in rough times. His contributions cannot be quantified and I will forever be grateful to him for making every bit of this thesis possible. I am thankful to Prof. Prमित Chowdhury for helping and supporting me in all my endeavours. This thesis has been buttressed by tremendous support from Prof. Sanjoy Bandyopadhyay (Department of Chemistry, IIT Kharagpur) who believed in me and consistently motivated me through his prompt emails. I cannot thank him enough for his boundless encouragement and determination to shape my research and letting me achieve new horizons. I express my deep sense of gratitude for Prof. M. Ali Haider (Department of Chemical Engineering) who mentored me with immense patience and knowledge. His consistent efforts to bring out the best in me and my work has fruitfully inspired my growth as a researcher. These people always had my best interests in mind and have been the substructures of this thesis. Their contributions extend much beyond the pages of this thesis and I am privileged to

complete my thesis under their guidance.

I thank my research committee members: Prof. Arunachalam Ramanan (Chairperson, SRC), Prof. Hemant Kashyap (Internal expert) and Prof. Pradipta Bandyopadhyay (External expert) for their timely evaluations. I would also like to thank Prof. Ravi Shankar (Head, Department of Chemistry), Prof. Narayanan Kurur (DRC Convenor, Chemistry) as well as the entire staff and faculty of Chemistry Department. I would also like to extend my thanks to Prof. Rajesh Khanna (Head, Department of Chemical Engineering). I thank IIT Delhi for financial support and for imbuing the best in me. I would also like to thank HPC facility at IIT Delhi for computational resources as well as HPC support team for their responsive emails and help. A special thanks to Prof. M. Ali Haider and Prof. Anurag S. Rathore for financial support. I am also thankful to all my teachers of St. Stephen's college who have been a constant source of motivation and inspiration in all these years.

I would also like to acknowledge the efforts and guidance of my first senior and brother, Dr. Manish Agarwal. His research insights and computing techniques since the nascent years of my summer project underpinned my skills and knowledge. I would also like to thank my best friend, Shruti and Satyam who were there to listen my ranting and raving at all times and to help me regain my focus in times of disgust. I am also thankful to my friends, Nidhi and Zeba who made my stay in IIT Delhi memorable with tea time talks and providing a change from the monotonous work schedule. I also thank Pramod bhaiya for always being there and giving me innumerable reasons to smile. I thank Abha aunty for her ladoos and for encouraging me all these years. I am also thankful to Anchal bhabhi who always believed that I will do great in life. I am also thankful to REC lab members for providing me a sense of belongingness in IIT Delhi and for all those parties and coffee times at CCD. A special thanks to Shelaka, Uzma and Fatimah for always telling me "Mam, sab ho jayega, chinta na karo". I also thank my other lab members for providing a competitive working environment. A very special thanks to my distant labmate, friend cum younger brother, Prabir who made my stay at IIT Kharagpur memorable and always went an extra mile to help and support me. I deeply cherish his quotes and messages that he used to send me to motivate me to never give up. A cardinal

role has been played by Saurav in all these years who stood by my side as a trenchant critique. I appreciate his research vision as well as his persistent efforts to transform me into a more practical and independent person. I am also thankful to his family for their unconditional love and care. A very special thanks to Saurav' mother for always keeping in touch and enquiring about my well-being. I would also express my love and gratitude towards my life saver, my car Nissan Micra who has protected and sheltered me in innumerable situations.

Above all, my words fail to express my gratitude towards my parents who have been the pillars of my life and have bestowed me with the strength and courage to stride towards making this day possible. I am truly blessed to have a wonderful and loving sister, Ritika who is my soul mate and can fight the world for me. Their uncountable support and motivation has always inspired my determination to sail in the boat of ambition with harbour as success. I am overwhelmed to thank my nani and nanaji who rooted my nerves with research. My nani has been the best grandmother one can have and a true source of inspiration who rejoiced with me when I was happy and to hold my back in times of hue. Her spiritual beliefs have further lightened my path with glory. I take this opportunity to thank God once again for giving me an awesome and encouraging family whose support and blessings embrace this thesis.

Madhulika Gupta

Date

Abstract

This thesis employs computer simulations to examine conformational preferences of peptides along the folding free energy landscape (FEL), role of hydration waters in mediating protein-glass transition and folding-unfolding equilibria, and deactivation of catalyst surfaces by biogenic impurities in fermentation derived feedstocks. As a first step to achieve this goal, we assess how small quantitative differences in different water models translate into significant dependence of conformational FEL for 20-residue, α -helical Trp-cage, on the choice of water models. The same set of water models generate qualitatively different secondary structure preferences for the unfolded peptide with a sequence-dependent response to the choice of water model. This study highlights the importance of adequate representation of peptide-water interactions to obtain better predictive values of biomolecular force fields, especially for the unfolded states. The effect of water models on the solvent-driven, protein-glass transition for Trp-cage is also examined. The correlated protein-water dynamics is unaffected by the choice of model, while the activation of methyl dynamics shows considerable sensitivity. The alterations induced in the folding pathway of 16-residue trpzips obtained by progressive substitution of hydrophobic core residues have been explored by performing replica exchange molecular dynamics simulations. The role of water in mediating protein-unfolding with sequential changes in hydration behaviour for encompassing set of metastable states with partially unfolded structures is outlined. Mutations modify packing of peptide backbone to adjust the changes in side chain volume, resulting in reshaping of the FEL for mutated peptides. The differential hydration behavior among the strand and turn regions of trpzips owing to their motional heterogeneity regulates the unfolding process. Finally, an approach towards understanding the physicochemical principles governing interactions and poisoning of metal surfaces by amino acids with varying side chain specificity is made by using steered molecular dynamics simulations. A bimetallic design of catalyst surface is examined to mitigate surface poisoning.

PERMISSIONS

Permissions have been taken from the respective journals for the publications related to work presented in this thesis.

List of Publications Related to Work Presented in this Thesis

1. **M. Gupta**, D. Nayar, C. Chakravarty and S. Bandyopadhyay, Comparison of Hydration Behaviour and Conformational Preferences of the Trp-cage Mini-protein in Different Rigid-Body Water Models, *Phys. Chem. Chem. Phys.*, **18**, 32796 (2016).
2. **M. Gupta**, C. Chakravarty and S. Bandyopadhyay, Sensitivity of Protein Glass Transition to the Choice of Water Model, *J. Chem. Theory Comput.*, **12**, 5643 (2016).
3. **M. Gupta**, T. S. Khan, S. Gupta, Md. I. Alam, M. Agarwal, M. A. Haider, Non-Bonding and Bonding Interactions of Biogenic Impurities with the Metal Catalyst and the Design of Bi-Metallic Alloys, *J. Catal.*, **352**, 542 (2017).
4. **M. Gupta**, P. Khatua, C. Chakravarty and S. Bandyopadhyay, The Sensitivity of Folding Free Energy Landscapes of Trpzip5 to Mutations in the Hydrophobic Core, *Phys. Chem. Chem. Phys.*, **19**, 22813 (2017).
5. **M. Gupta**, P. Khatua, C. Chakravarty and S. Bandyopadhyay, Hydration Behaviour along the Folding Pathway for Trpzip4, Trpzip5 and Trpzip6, *J. Phys. Chem. B*, (2018).
6. **M. Gupta**, T. S. Khan, M. Agarwal, M. A. Haider, Understanding the Nature of Amino Acid Interactions with Pd or Pd-Au Bimetallic Catalysts in the Aqueous Phase, *Langmuir*, (2018).

सार

इस थीसिस कंप्यूटर के सिमुलेशन को कन्सर संबंधी वरीयताओं की जांच करने के लिए कार्यरत हैं तह मुक्त ऊर्जा परिदृश्य (एफईएल), जलयोजन जल की भूमिका के साथ पेप्टाइड्स प्रोटीन कांच संक्रमण और तह-प्रबुद्ध संतुलन, और निष्क्रियकरण में मध्यस्थता में किण्वन व्युत्पन्न फीडस्टॉक में बायोजेनिक अशुद्धियों द्वारा उत्प्रेरक सतहों की। इस लक्ष्य को प्राप्त करने के पहले चरण के रूप में, हम आकलन करते हैं कि इसमें कितने छोटे मात्रात्मक अंतर हैं विभिन्न जल मॉडल, गठनात्मक एफ ए एल के महत्वपूर्ण निर्भरता में अनुवाद करते हैं पानी के मॉडल की पसंद पर 20-अवशेष, α - पेचदार ट्रिप - पिंजरे के लिए। का एक ही सेट पानी के मॉडल के लिए गुणात्मक रूप से भिन्न माध्यमिक संरचना प्राथमिकताएं उत्पन्न होती हैं पानी मॉडल की पसंद के अनुक्रम-आश्रित प्रतिक्रिया के साथ पेप्टाइड सामने आया। इस अध्ययन में पेप्टाइड-पानी के पर्याप्त प्रतिनिधित्व के महत्व पर प्रकाश डाला गया है बायोमोलेक्युलर फोर्स फील्ड्स के बेहतर भविष्य कहां प्राप्त करने के लिए इंटरैक्शन खुला राज्यों के लिए विलायक-संचालित, प्रोटेक्शनलास पर पानी के मॉडल का प्रभाव ट्रिप-पिंजरे के लिए संक्रमण की जांच भी की जाती है। सहसंबद्ध प्रोटीन-पानी की गतिशीलता मॉडल की पसंद से अप्रभावित है, जबकि मिथाइल गतिशीलता का सक्रियण काफी संवेदनशीलता दिखाती है तह के मार्ग में प्रेरित परिवर्तन हाइड्रोफोबिक कोर अवशेषों के प्रगतिशील प्रतिस्थापन द्वारा प्राप्त 16-अवशेषों ट्रिपज़िप प्रतिकृति विनिमय आणविक गतिशीलता सिमुलेशन के प्रदर्शन से पता लगाया गया है। जलयोजन में अनुक्रमिक परिवर्तन के साथ प्रोटीन-खुलासा में मध्यस्थता में पानी की भूमिका आंशिक रूप से सामने आने वाले महानतम राज्यों के सेट को शामिल करने के लिए व्यवहार संरचनाओं को रेखांकित किया गया है। उत्परिवर्तन समायोजित करने के लिए पेप्टाइड रीढ़ की पैकिंग को संशोधित करता है साइड चेन वॉल्यूम में परिवर्तन, जिसके परिणामस्वरूप उत्परिवर्तित के लिए एफईएल के पुनर्निर्धारण में हुई पेप्टाइड्स। किनारा और मोड़ के क्षेत्रों में अंतर हाइड्रेशन व्यवहार उनकी गति विविधता के कारण ट्रिपज़िप खुलासा प्रक्रिया को नियंत्रित करता है। आखिरकार, भौगोलिक रासायनिक सिद्धांतों को समझने की दिशा में एक दृष्टिकोण विभिन्न साइड चेन के साथ अमीनो एसिड द्वारा धातु की सतहों की बातचीत और विषाक्तता विशिष्टता को स्टीयरेड आणविक गतिशीलता सिमुलेशन का उपयोग करके बनाया गया है एक बाईमेटेलिक सतह के विषाक्तता को कम करने के लिए उत्प्रेरक की सतह के डिजाइन की जांच की जाती है।

Contents

Certificate	i
Acknowledgements	iii
Abstract	vii
Permissions	ix
Table of Contents	xi
List of Figures	xv
List of Tables	xxvii
1 Introduction	1
1.1 Peptides and Proteins	2
1.2 Hydration of Proteins and Hydration Shell Behaviour	4
1.3 Protein Folding and Unfolding	6
1.3.1 Secondary Structures	7
1.3.2 Thermodynamics and Kinetics of Protein Unfolding	12
1.3.3 Free Energy Landscape	19
1.4 Protein-Glass Transition	23
1.5 Proteins as Inhibitors on Metal Catalysts	26
1.6 Systems of Interest	29
1.6.1 Trp-cage	29
1.6.2 Trpzips: Mutants of β -hairpin	30
1.6.3 Amino Acids and Peptides as Biogenic Impurities	32

1.7	Motivation and Organization of Thesis	33
2	Methods and Computational Details	39
2.1	Ensembles	40
2.1.1	Microcanonical Ensemble	41
2.1.2	Canonical Ensemble	42
2.1.3	Isothermal-Isobaric Ensemble	44
2.2	Potential Energy Models	44
2.2.1	Types of Intermolecular Interactions	45
2.2.2	Water	48
2.2.3	Proteins	52
2.2.4	Water-Protein Interactions	56
2.2.5	Metals as Catalyst	57
2.3	Molecular Dynamics (MD) Simulations	59
2.3.1	Integration Algorithms	60
2.3.2	Thermostat and Barostat	62
2.3.3	RATTLE and SHAKE	65
2.4	Periodic Boundary Conditions and Short Range Forces	66
2.5	Treatment of Long-Range Forces	68
2.5.1	Ewald Summation	69
2.5.2	Particle Mesh Ewald	72
2.6	Efficient Sampling Techniques	74
2.7	Non-Equilibrium Dynamics	78
3	Comparison of Hydration Behavior and Conformational Preferences of Trp-cage Mini-protein in Different Rigid-body Water Models	83
3.1	Computational Details	88
3.2	Observables	90
3.2.1	Order Metrics for the Peptide Secondary Structure	91
3.2.2	Hydration Shell Metrics	93
3.2.3	Criteria for Characterization of Folded and Unfolded States	94

3.3	Results and Discussion	94
3.3.1	Tetrahedral Order of Water Models in Bulk	94
3.3.2	Unfolding Transition	96
3.3.3	Secondary Structure Metrics in the Folded and Unfolded Ensembles	98
3.3.4	Structure of the Hydrophobic Core	104
3.3.5	Hydration Shell Structure and Energetics	106
3.3.6	Residue-wise Decomposition of Configurational Energies	109
3.4	Errors and Simulation Time Scales	112
3.5	Summary and Conclusions	114
4	Sensitivity of Protein Glass Transition to the Choice of Water Model	117
4.1	Simulation Details	119
4.2	Results	121
4.2.1	Onset of Anharmonicity	121
4.2.1.1	Root Mean Square Fluctuations of Protein	121
4.2.1.2	Mean Square Displacement of Protein	122
4.2.1.3	Mean Square Displacement of Hydration Water	123
4.2.1.4	Hydrogen Bond Network	124
4.2.2	Water Ordering in the Hydration Shell	125
4.2.3	Contribution of Individual Residues of Trp-Cage to Anharmonicity	132
4.2.4	Methyl Rotations at 150 K	134
4.3	Conclusions	139
5	Mapping out Free Energy Landscapes of Trpzip4, Trpzip5 and Trpzip6 and Their Hydration Behavior along the Folding Pathway	141
5.1	Methodology	147
5.2	Equilibrium and Convergence of REMD Simulations	148
5.3	Results	151
5.3.1	Fraction Folded Analysis	151

5.3.2	Thermodynamic Stability of the Trpzip	153
5.3.3	Principal Component Analysis	154
5.3.4	Secondary Structure Order Metrics	156
5.3.5	Residue-wise Interaction Energies	163
5.3.6	Proposed Mechanism of Trpzip Folding	165
5.3.7	Water Structure and Ordering	168
5.3.8	Water Dynamics	173
5.3.8.1	Translational Motion	174
5.3.8.2	Rotational Motion	176
5.3.9	Hydrogen Bond Dynamics	179
5.4	Conclusions	184
6	Deactivation of Ni (111) and Pd (111) Surfaces by Amino Acids	189
6.1	Computational Methods	192
6.2	Results	196
6.2.1	Ni (111) Surface	196
6.2.2	Pd (111) Surface	207
6.3	Conclusions and Outlook	222
7	Conclusions	227
	Bibliography	233
	Biodata of the Candidate	

List of Figures

1.1	Structures of all twenty naturally occurring amino acids. Adapted from reference [16].	2
1.2	Schematic representation of hierarchy in protein structure. Adapted from reference [2] with permission.	3
1.3	(a) Atoms involved in formation of the dihedral angles (ϕ, ψ) by the peptide backbone atoms [57], (b) Ramachandran plot demarcating regions for different secondary structures.	8
1.4	Spectra obtained from circular dichroism (CD) experiments distinguishing different secondary structures present in a protein. The y axis unit represents a simplified version of the units used in CD spectroscopy. The figure is adapted from reference [1].	9
1.5	Thermal denaturation curve for Trp-cage as obtained from NMR and CD experiments using different solvents at physiological pH. The melting transition midpoint in 42° in aqueous phase at pH=7. The figure has been adapted with permission from reference [61].	13
1.6	Protein Stability Curve. The slope and curvature give the change in entropy and heat capacity on unfolding, respectively. T_h , T_s and T_u denote the temperatures at which ΔH , ΔS and ΔG , respectively, are equal to zero. A schematic of triangular relationship between $T_s - T_h$ and ΔG is also shown. The figure is adapted with permission from reference [63].	15

1.7	Heat capacity change on unfolding of Trp-cage peptide as a function of temperature as obtained from differential scanning calorimetry. $C_{p,U}$ and $C_{p,N}$ represent the baselines for heat capacities of peptide in the unfolded and native states, respectively. The figure has been adapted with permission from reference [64].	17
1.8	Schematic representation of “funnel-like” free energy landscape. The figure is adapted from reference [1].	20
1.9	Protein-glass transition as measured by temperature dependence of Debye-Waller factor of heavy atoms of ribonuclease A protein. The figure is adapted with permission from reference [48].	24
1.10	Proposed reaction routes for the metal catalyzed hydrogenation (black arrow), and hydrodeoxygenation (red arrow) and aqueous phase system reforming (blue arrow) of fermentation-derived platform molecules.	28
2.1	Contours of total electron density of water molecule in HOH plane as obtained from quantum mechanical calculations [198].	49
2.2	Schematic representation of rigid body water models.	50
2.3	Fraction of population with (a) α -helix, $F_{\alpha-helix}$, (b) β -sheet, $F_{\beta-sheet}$, and PPII regions, F_{PPII} as a function of temperature. MG and Literature represent the data obtained from my simulations and as given in reference [151], respectively.	78
2.4	(a) Pictorial representation of stacking of water molecules above Ni (111) surface. (b) Water density profile for Pd (111) and Ni(111) surfaces.	80

3.1	Cartoon representation of Trp-cage peptide with different secondary structure elements highlighted with different colours. Ramachandran plot depicting the prominent regions occupied by the peptide in the folded state in mTIP3P water model are also shown. Residues 2-8 form the right handed alpha-helix(α_R) (purple), residues 11-14 form 3_{10} helix (blue), and Proline 17-19 are visible in the Polyproline II (PPII) (red) region of the Ramachandran plot. Glycines 10, 11, and 15 are shown in green. Residues 9 and 16 form the salt-bridge which are shown in orange in the cartoon representation of the peptide.	85
3.2	Normalized conditional probability distributions of tetrahedral order, $P_n(q_{tet})$ for water molecules with coordination number (n) at 250 K, 1.00 g cm^{-3} for (a) mTIP3P, (b) TIP4P, and (c) TIP4P-Ew. The inset figure shows coordination number distributions, $P(n)$ as a function of n computed at 250 K, 1.00 g cm^{-3} for the respective water models. The color coding used for different n in inset is same as in the main figure.	95
3.3	Temperature dependent behavior of order metrics (a) number of native contacts, $\langle N_{nc} \rangle$, of the peptide, (b) radius of gyration, $\langle R_g \rangle$, of the full peptide, (c) radius of gyration, $\langle R_{core} \rangle$, of the hydrophobic core, and (d) root mean square deviation, $\langle RMSD \rangle$, of the heavy atoms of the peptide in different water models. Blue and yellow color show the range of the order metrics corresponding to the folded and unfolded ensembles, respectively.	97
3.4	Contour plots of the two dimensional probability distributions as a function of end to end distance, (D_{end}) and number of hydrogen bonds, (N_{HB}) for the peptide in (a), (b), (c) F state; (d), (e), (f) U1 state; (g), (h), (i) U2 state; (j), (k), (l) U3 state; (m), (n), (o) U4 state; (p), (q), (r) U5 state solvated in mTIP3P, TIP4P, and TIP4P-Ew around 250 K.	99

3.5	Contour plots of the two dimensional probability distributions as a function of radius of gyration (R_g) and root mean square deviations from the native folded structure (RMSD) for the peptide in (a), (b), (c) F state; (d), (e), (f) U1 state; (g), (h), (i) U2 state; (j), (k), (l) U3 state; (m), (n), (o) U4 state; (p), (q), (r) U5 state solvated in mTIP3P, TIP4P, and TIP4P-Ew around 250 K.	101
3.6	Contour plots of the probability distributions of Ramachandran angles of the full peptide in folded and unfolded ensembles in the (a), (b), (c) F state; (d), (e), (f) U1 state and (g), (h), (i) U2 state, solvated with mTIP3P, TIP4P, and TIP4P-Ew water models, respectively, around 250 K.	103
3.7	Contour plots of the probability distributions of Ramachandran angles of the hydrophobic core residues of the folded and unfolded ensembles of the peptide in (a), (b), (c) Folded state; (d), (e), (f) U1 state; (g), (h), (i) U2 state; (j), (k), (l) U3 state; (m), (n), (o) U4 state and (p), (q), (r) U5 state in mTIP3P, TIP4P, and TIP4P-Ew water models, respectively, around 250 K.	105
3.8	Local hydration shell properties, (a) average number of waters, $n(r)$ (b) average local tetrahedral order of waters, $q_{tet}(r)$ and (c) average binding energy of waters, $u_{tag}(r)$ as a function of distance from Trp-cage in the folded and unfolded ensembles around 250 K. Red, blue, and green colors indicate peptide solvated in mTIP3P, TIP4P, and TIP4P-Ew water models, respectively.	107
3.9	Temperature dependent variation of (a) average number of water molecules ($\langle n_{wat}^{first} \rangle$) and (b) average tetrahedral order ($\langle q_{tet}^{first} \rangle$) of water molecules in the first hydration shell of the peptide solvated in mTIP3P, TIP4P, and TIP4P-Ew. The error bars are smaller than the point symbol size.	108

3.10	Interaction energy of each of the amino acid residues of the peptide with (a) all the other residues of peptide and waters around the peptide ($u_{res-all}$), (b) all the other residues of the peptide ($u_{res-res}$), (c) all the water molecules in the solvated system ($u_{res-wat}$), (d) shows binding energy, (u_{res}) of water molecules in the first hydration shell of each residue in the folded and unfolded ensembles of the peptide in mTIP3P, TIP4P, and TIP4P-Ew around 250 K. The standard errors associated are within 3 %.	110
4.1	(a) Root mean square fluctuations, $\langle RMSF \rangle$ of the non-hydrogen atoms of the peptide with respect to time averaged conformations, (b) Mean square displacements of non-hydrogen atoms of the protein, $\langle MSD_{protein} \rangle$ over 100 ps durations, (c) Mean square displacement of water molecules in the first hydration shell of the peptide, $\langle MSD_{water} \rangle$ over 10 ps durations as a function of temperature in mTIP3P, TIP4P and TIP4P-Ew water models.	122
4.2	Average number of (a) peptide-water hydrogen bonds, $\langle N_{HB}^{PW} \rangle$ and (b) water-water hydrogen bonds, $\langle N_{HB}^{WW} \rangle$ as a function of temperature in mTIP3P, TIP4P and TIP4P-Ew water models.	125
4.3	Comparison of the average number of water molecules, $n(r)$, as a function of distance from Trp-cage mini-protein solvated in (a), (b) mTIP3P; (c), (d) TIP4P and (e), (f) TIP4P-Ew water models.	126
4.4	Comparison of tetrahedral order of waters, $q_{tet}(r)$, as a function of distance from the peptide solvated at different temperatures in (a), (b) mTIP3P; (c), (d) TIP4P and (e), (f) TIP4P-Ew water models.	127
4.5	Normalized distributions of tetrahedral order of waters, $P_r(q_{tet})$, lying between a distance of r and $r + \delta r$ ($r = 1.75 \text{ \AA}$, $\delta r = 0.25 \text{ \AA}$) from the peptide solvated at different temperatures in (a), (b) mTIP3P; (c), (d) TIP4P and (e), (f) TIP4P-Ew water models.	128

4.6	Normalized distributions of tetrahedral order of waters, $P_r(q_{tet})$, lying between a distance of r and $r + \delta r$ ($r = 2.75 \text{ \AA}$, $\delta r = 0.25 \text{ \AA}$) from the peptide solvated at different temperatures in (a), (b) mTIP3P; (c), (d) TIP4P and (e), (f) TIP4P-Ew water models.	129
4.7	Normalized distributions of tetrahedral order of waters, $P_r(q_{tet})$, lying between a distance of r and $r + \delta r$ in the first hydration shell of the peptide at $r = 4.0 \text{ \AA}$, $\delta r = 0.25 \text{ \AA}$ for (a), (b) mTIP3P water model and at $r = 4.5 \text{ \AA}$, $\delta r = 0.25 \text{ \AA}$ for (c), (d) TIP4P and (e), (f) TIP4P-Ew water models solvated at different temperatures.	130
4.8	Temperature dependent variation of (a) average number of water molecules, $\langle n_{wat}^{first} \rangle$ and (b) average tetrahedral order, $\langle q_{tet}^{first} \rangle$ of water molecules in the first hydration shell of the peptide solvated in mTIP3P, TIP4P and TIP4P-Ew water models.	132
4.9	Mean square displacements, MSD for individual residues (non-hydrogens) of the peptide over 100 ps durations as a function of temperature solvated in (a), (b) mTIP3P; (c), (d) TIP4P and (e), (f) TIP4P-Ew water models.	133
4.10	Probability density maps for some of the tagged methyl proton around its carbon at 150 K for Trp-cage peptide in different water models. C1 represents the methyl carbon, C2 denotes the carbon bonded to methyl carbon and C3 represents the next adjacent carbon. C1 atom in grey and orange color denotes either of the C_ϵ for Leu2 (L) residue, red and yellow denotes either of the C_ϵ for Leu7 (L') residue, while purple color denotes the C_ϵ for Ile4 residue. For representative purpose, the 'unimodal', 'bimodal' and 'trimodal' distributions are marked in one frame in each case.	136
4.11	Histograms of probability density maps, $P_{methyl-H}$, of tagged methyl protons of Trp-cage at (a) 130 K, (b) 150 K, (c) 170 K and (d) 220 K in mTIP3P, TIP4P and TIP4P-Ew water models. $P_{methyl-H} > 3$ corresponds to delocalized distributions.	138

5.1	(a-c) Root mean square deviations, RMSD and (d-f) d_{RMS} as a function of time for TZ4, TZ5 and TZ6 at 300 K. The black line shows the average over 5 ns window.	148
5.2	Mixing parameter, $m(T)$ as a function of temperature for TZ4, TZ5 and TZ6.	149
5.3	(a-c) Energy histograms, (d-f) ratio of histograms, $\ln[H(E, T_{i+1})/H(E, T_i)]$ (symbols) and least-squares fit corresponding to Boltzmann distributions (solid lines) for TZ4, TZ5 and TZ6. Red color indicates the first replica corresponding to temperature of 250 K followed by other replicas up to 550 K.	151
5.4	Fraction of folded populations, ρ_F of TZ4, TZ5 and TZ6 as a function of temperature.	152
5.5	Free energy contour maps (in units of $k_B T$) as a function of the principal components, PC1 and PC2 for (a) TZ4, (b) TZ5 and (c) TZ6 at 300 K.	155
5.6	Free energy contour maps (in units of $k_B T$) of two dimensional probability distributions as a function of root mean square deviations with respect to the equilibrated structure and radius of gyration for (a-c) non-hydrogen atoms, (RMSD and R_g), (d-f) C_α atoms (RMSD $_\alpha$ and R_α) of all the residues of TZ4, TZ5 and TZ6 at 300 K.	157
5.7	Free energy contour maps (in units of $k_B T$) of two dimensional probability distributions as a function of root mean square deviations with respect to the equilibrated structure and radius of gyration for the hydrophobic core residues (RMSD $_{core}$ and R_{core}) of (a) TZ4, (b) TZ5 and (c) TZ6 at 300 K.	159

5.8	Free energy contour maps (in units of $k_B T$) of two dimensional probability distributions as a function of (a-c) root mean square deviation of the turn residues (RMSD_{turn}) and distance between centers of mass of side chains of residues 5 and 12 (d(5,12)), (d-f) root mean square deviation of the strand residues ($\text{RMSD}_{strands}$) and distance between centers of mass of side chains of residues 5 and 14 (d(5,14)) for TZ4, TZ5 and TZ6 at 300 K.	161
5.9	Interaction energy of each residue of trpzip with the other residues present in the peptides, $u_{res-res}$ in the folded and unfolded ensembles of (a) TZ4, (b) TZ5 and (c) TZ6 at 300 K.	164
5.10	Schematic representation of the folding free energy pathway for Trpzip4, Trpzip5 and Trpzip6.	166
5.11	Free energy contour maps (in units of $k_B T$) of Ramachandran angles (ϕ, ψ) for folded (F) and unfolded (U1-U4) ensembles of TZ4 at 300 K.	167
5.12	Free energy contour maps (in units of $k_B T$) of Ramachandran angles (ϕ, ψ) for folded (F) and unfolded (U1,U2) ensembles of (a-c) TZ5 and (d-f) TZ6 at 300 K.	168
5.13	Average number of waters in the first hydration shell of the peptide (n_{wat}^{first}) around different segments of TZ4, TZ5 and TZ6 in the folded and unfolded ensembles.	170
5.14	Average local tetrahedral order (q_{tet}^{first}) and average binding energy (u_{tag}^{first}) of waters in the first hydration shell around different segments of TZ4, TZ5 and TZ6 in the folded and unfolded ensembles.	171
5.15	Interaction energy of each of the amino acid residues of the peptide with (a-c) all the water molecules in the solvated system, $u_{res-wat}$, and (d-f) all the other residues of peptide and waters around the peptide ($u_{res-reswat}$), of TZ4, TZ5 and TZ6 in the folded and unfolded ensembles.	173
5.16	Diffusion coefficient (D) of waters present in the first hydration layers of different segments of TZ4, TZ5 and TZ6 in the folded and unfolded ensembles.	175

5.17	Average reorientational time constants ($\langle\tau_{\mu}\rangle$) of water present in the first hydration layers of different segments of TZ4, TZ5 and TZ6 in the folded and unfolded ensembles.	178
5.18	Average relaxation times of intermittent (a-c) PW ($\langle\tau_C^{PW}\rangle$) and (d-f) WW ($\langle\tau_C^{WW}\rangle$) hydrogen bond TCFs for water present in the hydration layer around different segments of TZ4, TZ5 and TZ6 in the folded and unfolded ensembles.	180
5.19	Average relaxation times of continuous (a-c) PW ($\langle\tau_S^{PW}\rangle$) and (d-f) WW ($\langle\tau_C^{WW}\rangle$) hydrogen bonds TCFs for water present in the hydration layer around different segments of TZ4, TZ5 and TZ6 in the folded and unfolded ensembles.	182
6.1	Potential interaction sites for respective amino acids. A representative structure for amino acids is shown with backbone atoms as interaction sites. The interaction sites or tagged sites in SMD simulations are shown in blue color for each amino acid.	194
6.2	Orientations of amino acids and Cys-dimer studied for non-bonded interaction with the Ni (111) surface via the preferential site as calculated from SMD simulations.	198
6.3	PMF profile as a function of z coordinate for preferential adsorbing sites for (a) Ala and S-containing amino acids (Cys, Met), (b) aromatic amino acids (Trp and His), (c) miscellaneous amino acids (Lys, Thr and Glu) and (d) Cys-dimer on Ni(111) surface as calculated from SMD simulations.	199
6.4	Interaction energy, E_{int} , as a function of z coordinate for all the SMD runs performed for each adsorbing site for all the amino acids. In addition, solvent density profiles as a function of z coordinate for Ni (111) surface are also plotted.	201
6.5	Top view of the flat orientations of (a) Trp and (b) His on the Ni (111) surface as observed in MD simulations.	202

6.6	Solvent accessible surface area (SASA) as a function of calculated non-bonded interaction energy (E_{int}) for all the amino acids studied on Ni (111) surface as calculated from MD simulations. The values are linearly fitted with a correlation coefficient of 0.94.	206
6.7	Interaction energy, E_{int} as a function of z coordinate for all the SMD runs performed for each potential interacting site for all the amino acids. In addition, solvent density profiles as a function of z coordinate for Pd(111) surface are also plotted on y2 axis.	207
6.8	Orientations of S-containing amino acids (a) Cys, (b) Met and aliphatic amino acids (c) Gly, (d) Ala, (e) Leu (f) Pro on Pd(111) surface. The distances of preferential interaction site from the top of the metal surface are also indicated in each case.	210
6.9	PMF profile as a function of z coordinate for the interacting sites for (a) S-containing amino acids (Cys, Met), (b) Aliphatic amino acids (Gly, Ala, Leu and Pro), (c) Aromatic amino acids (Trp, His, Phe and Tyr), and (d) Polar amino acids (Thr, Lys, Arg, Glu and Gln) on Pd(111) surface.	211
6.10	Positioning of S atom (yellow color) of Met as observed in five different simulations used for calculating the average E_{int} value on (a) Pd (111) surface, (b) Pd-Au uniform, (c) Pd-Au strips, (d) Pd-Au single island and (e) Pd-Au multiple islands. The tan and red colors indicate Pd and Au atoms, respectively.	212
6.11	Variation of interaction energy, E_{int} , with the increase in coverage for Met interacting with the Pd (111) and different Pd-Au segregated surfaces.	214
6.12	Orientations of aromatic amino acids (a) Trp, (b) His, (c) Phe (d) Tyr and polar amino acids (e) Thr, (f) Lys, (g) Arg, (h) Glu and (i) Gln on Pd(111) surface. The distances of preferential interaction site from the top of the metal surface are also indicated in each case. . . .	216

6.13	Solvent accessible surface area, SASA as a function of interaction energy, E_{int} , via the preferential interaction site for each amino acid as obtained from MD simulations. The values are fitted using a straight line which is shown in red.	221
6.14	Diffusion coefficient, D, as a function of interaction energy, E_{int} , via the preferential interaction site for each amino acid, as obtained from MD simulations. The values of diffusion coefficient are calculated by splitting the trajectory into blocks of 100 ps.	222
6.15	Summary of experimental and theoretical results. The inner circle depicts the experimental observation in previous reports [126, 131], while the outer circle depicts the theoretically calculated interacting site and mode of deactivation in this study.	223

List of Tables

1.1	The values for dihedral angles (ϕ, ψ) for various secondary structure conformations of peptides classified in the Ramachandran plot. This table has been taken from reference [59].	10
1.2	Sequence of trpzip3. The hydrophobic core residues are highlighted in blue color. The mutations induced with respect to Trpzip4 are stated along with their unfolding temperatures (T_m) and grand average hydrophathy index (HI) [167].	32
2.1	Potential energy parameters of RB water models [185, 199, 202, 203]. ϵ and σ denotes the well-depth and length scale parameter, respectively, where the subscripts OO, HH and OH denote distinct pair interactions between atomic sites. The charges on oxygen, hydrogen atoms, and massless site are denoted by q_O , q_H , q_M , respectively. The oxygen-hydrogen and oxygen-massless site distance are denoted by r_{OH} and r_{OM} , respectively, and H-O-H is the bond angle.	51
2.2	Lattice constants, energy (ϵ) and size parameters (σ) and solid-water interfacial tension ($\gamma_{SL}^{(111)}$) for some metals as given in CHARMM-METAL force field [174].	58
2.3	Comparison of ensemble average potential energy from conventional MD simulations (NVT and NVE ensembles) and REMD simulations (NVT ensemble). The values compare well with the literature [240] within the standard deviation reported in latter.	78

3.1	Properties of the bulk solvents at 300 K and 1.0 g cm ⁻³ . Configurational energy (U_{conf}), electrostatic energy (U_{elec}), and Lennard-Jones contributions to the potential energy per molecules (U_{vdw}) are calculated in kJ mol ⁻¹ . Hydrogen bonding strength (E_{HB}) has been calculated for the water dimer as stated in reference [277]. Tetrahedral order ($\langle q_{tet} \rangle$), dipole moment (μ in units of D), quadrupole moment (Q_T in units of D-Å), ratio of dipole-quadrupole moments (μ/Q_T in units of Å ⁻¹), relative dielectric constant (ϵ_r) and self diffusion coefficient (D in units of 10 ⁻⁵ cm ² s ⁻¹), are also reported for different solvent models [199, 200, 203, 277, 278].	87
3.2	Simulation protocol describing the run lengths for equilibration (t_E) and production (t_P) runs performed in NPT and NVE ensembles, respectively.	89
3.3	Average temperature, configurational energy, and density of the system for the folded and unfolded ensembles obtained after quenching at five different listed rates with respective water models.	90
3.4	Order parameters for temperatures below and above the unfolding transition for Trp-cage solvated with different water models. Extended simulations upto 50 ns are denoted by asterisk.	96
3.5	Ensemble average values of order metrics for full peptide computed by considering non-hydrogen atoms of the peptide in the folded and unfolded ensembles in mTIP3P, TIP4P, and TIP4P-Ew around 250 K. The unit of length is Å, S_{conf} is reported in JK ⁻¹ mol ⁻¹ , and SASA is reported in (Å ²).	100
3.6	Order metrics for hydrophobic core residues in the folded and unfolded ensembles of the peptide solvated by mTIP3P, TIP4P, and TIP4P-Ew around 250 K. Standard errors for $U_{core-wat}$ is denoted in parenthesis.	106
3.7	Average number of water molecules in the first hydration shell of the peptide for folded and unfolded ensembles solvated in mTIP3P, TIP4P, and TIP4P-Ew around 250 K.	108

3.8	Different order parameters for the variants of U1 state solvated with different water models around 250 K. U1 refers to ensemble averaged values over 20 ns run length, while U1* refers to ensemble averaged values by extending the former run upto 100 ns. U1a and U1b refers to additional unfolded ensembles around 250 K obtained after repetitive quenching from the same initial configuration at respective high temperatures. Helical content is found to be zero for all these states in all the water models. The errors are denoted in the parentheses.	113
5.1	Sequence and hydrophathy values [167] for each segment in TZ4, TZ5 and TZ6.	146
5.2	Thermodynamic parameters of unfolding for TZ4, TZ5 and TZ6. Comparison of experimental data [152] with the data obtained from thermodynamic fit of the melting curve in our work using CHARMM36 force field.	154
5.3	Ensemble average values of different secondary structural order metrics (in \AA units) for TZ4, TZ5 and TZ6. The standard errors in all the computed quantities are less than 2 and 8 % for folded and unfolded ensembles, respectively.	160
5.4	Ensemble Average Values of Some More Order Metrics for TZ4, TZ5 and TZ6. The standard errors vary from 0.5-1 % for SASA and SASA _{core} for the folded ensembles and 9-12 % for unfolded ensembles. d(5,12) and d(5,14) have standard errors of less than 10%.	162
6.1	Comparison of interaction energies, E_{int} (in kJ/mol) through the preferential interaction for different amino acids on Ni (111) surface by averaging over the best 5, 7 and 10 interaction energies as calculated from SMD simulations. The values in the brackets denote standard errors.	195
6.2	Interaction energies, E_{int} (kJ/mol) between the preferential interacting site of Cys and Ni (111) surface by averaging over best 5 interaction energies from 3 independents sets of 20 SMD runs.	196

6.3	Interaction energies, E_{int} (kJ/mol) between the preferential interacting site of Cys and Ni (111) surface by averaging over best 5 interaction energies with different sample sizes (SS) of SMD runs.	196
6.4	Interaction energy, E_{int} (kJ/mol) and distance, D_{int} (\AA) between the interacting site and the top metal surface, for the backbone atoms of all the amino acids and Cys-dimer on Ni (111) surface as calculated from SMD simulations. The values in brackets denote the standard error.	197
6.5	Interaction energy, E_{int} (kJ/mol) and distance, D_{int} (\AA) between the interacting site and the top metal surface, for the side chain sites of all the amino acids and Cys-dimer on Ni (111) surface as calculated from SMD simulations. The values in brackets denote the standard error in the respective values.	197
6.6	Interaction energies, E_{int} (kJ/mol) for the backbone atoms of the amino acids and distance between the interacting site and the top metal surface, D_{int} (\AA) for different amino acids on Pd (111) surface. The values in brackets denote the standard error in calculations. . . .	208
6.7	Interaction energies, E_{int} (kJ/mol) for the side chain atom(s) of the amino acids and distance between the interacting site and the top metal surface, D_{int} (\AA) for different amino acids on Pd (111) surface. The values in brackets denote standard error.	209
6.8	Interaction energies, E_{int} (kJ/mol) for Met on different surfaces. The values in brackets denote the standard error in calculations. The distance between the S atom of Met and the listed metal surface is 3.1 \AA	212